Scheme V

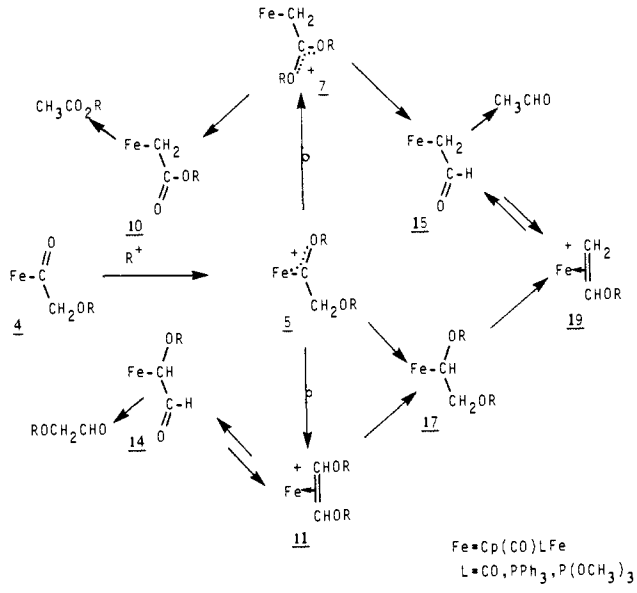

Scheme V are numbered as their Fp derivatives.) Carbocationic alkylating agents convert **4** into its α,β-dialkoxyethylidene complexes **5**, which can be reduced to the α,β-dialkoxyethyl compounds **17** (isolated for L = CO). These then convert either directly (L = PPh_3, $P(OCH_3)_3$) or indirectly via isolable **19** (L = CO) into their respective formylmethyl derivatives **15** and then (after protonating) acetaldehyde. Alternatively, **5** may rearrange to the (η^2-1,2-dialkoxyethylene) complex **11** (L = CO); this in turn provides its η^1-methoxyformylmethyl compound **14**, then methoxyacetaldehyde (after hydrolysis, protonation) or **17** (after reduction). Protonating **4** on the other hand delivers a α-hydroxy-β-methoxyethylidene salt that subsequently isomerizes to its ketene hemiacetal complex **7** [L = CO, PPh_3, $P(OMe)_3$]. These afford the carbalkoxymethyl ligand on **10**, which is a precursor to **15** or to methylacetate.

Complexes $FpCH(OR)CH_2OCH_3$ **17** and **18**, obtained by reducing either **5** or **11**, are stable once purified. Certainly, they are no less stable than other Fp-η^1-alkyl complexes bearing β-alkoxy substituents (e.g., **27** and **28**); all degrade or react with electrophiles via β-alkoxide cleavage. This β-alkoxide lability for **17** and **18** does not presage their isomerizing to formylmethyl acetal complexes **27** (eq 17), however. We must emphasize that analogous α,β-dihydroxyethyl complexes **3**, as with other α-hydroxyalkyl compounds,[52] should prove to be much less stable by virtue of having alternative degradation pathways available. They could, for example, homolytically cleave the metal–carbon σ-bond and generate a hydroxyalkyl radical $RCH(OH)^{\bullet}$,[47] or they could deinsert metal–hydride[2]—both reactions ultimately give free aldehyde. Nevertheless, it is conceivable that α,β-dialkoxyethyl complexes **17** and **18**, or other protected forms of α,β-dihydroxyethyl complexes **3**, could chain extend by successively incorporating CO, activating (with organic or other electrophiles), and then reducing the new acyl to homologous α, β, γ,··· alkoxyalkyl derivatives.[53] Work is in progress toward this goal using labile cobalt–carbonyl systems.

Acknowledgment. Exploratory studies were carried out when two of the authors (T.W.B. and A.R.C.) were at Wesleyan University (Department of Chemistry), Middletown, CT. Support from the Department of Energy, Office of Basic Energy Sciences, is gratefully acknowledged.

(52) Selover, J. C.; Vaughn, G. D.; Strouse, C. E.; Gladysz, J. A. *J. Am. Chem. Soc.* **1986**, *108*, 1455. Vaughn, G. D.; Strouse, C. E.; Gladysz, J. A. *J. Am. Chem. Soc.* **1986**, *108*, 1462.

(53) In related studies, Stimson and Shriver converted $(CO)_5MnCH_3$/CO/BH_3 to mixtures of C_1–C_4 alkenes and alkanes. Chain growth entailed BH_3 reduction of an acyl to its homologous saturated alkyl, which then inserted CO. Stimson, R. E.; Shriver, D. F. *Organometallics* **1982**, *1*, 787.

Biphasic Kinetics and Temperature Dependence of Iron Removal from Transferrin by 3,4-LICAMS

Suzanne A. Kretchmar and Kenneth N. Raymond*

Contribution from the Department of Chemistry, University of California, Berkeley, California 94720. *Received March 3, 1986*

Abstract: The kinetics of iron removal from transferrin by the synthetic catechol sequestering agent *N,N',N''*-tris(5-sulfo-2,3-dihydroxybenzoyl)-1,5,10-triazadecane (3,4-LICAMS) have been investigated at pH 7.4 and a range of temperatures. In contrast to an earlier report, biphasic kinetics are observed for iron removal from diferric transferrin. This is attributed to kinetic inequivalence between the two sites, and the absorbance–time curves are fit to a model incorporating this assumption. Elucidation of the two observed macroscopic rate constants is achieved by exclusively labeling the individual sites of the protein with ^{55}Fe or ^{59}Fe. At 25 °C iron is removed from the N-terminal site at approximately twice the rate as from the C-terminal site. The two microscopic rate constants agree within experimental error with those obtained from the first-order processes of iron removal from N-terminal and C-terminal monoferric transferrins. The activation enthalpy for iron release from C-terminal monoferric transferrin by 3,4-LICAMS is 20 (1) kcal/mol over the entire range 4–20 °C. The corresponding values for N-terminal monoferric transferrin are 21 (2) kcal/mol below 20 °C and 15 (1) kcal/mol above 20 °C. These activation enthalpies agree with the observation that the rates of iron removal from the two monoferric transferrins are similar in the low-temperature regime but differ by a factor of about 2 in the high-temperature regime. It is proposed that the N-terminal site undergoes a conformational change at 20 °C which results in more facile iron release at physiological temperature.

Serotransferrin, the iron transport protein found in blood serum, has been well characterized.[1-4] The protein is bilobal, and each lobe contains an iron-binding site. Estimates of the metal–metal distance indicate that the sites are too distant (35 nm) for direct interaction.[1,5] Although similar, the two sites are not chemically identical.[6,7] For example, the C-terminal site has three more

* Author to whom correspondence should be addressed.

(1) Chasteen, N. D. *Advances in Inorganic Biochemistry*; Thiel, E. C., Eichorn, G. L., Marzilli, L. G., Eds.; Elsevier: New York, 1983; Vol. 5, pp 201–233.

0002-7863/86/1508-6212$01.50/0

cystine bridges and is more acid-stable than the N-terminal site.[1,7] These properties have been exploited for selectively labeling the C-terminal and N-terminal sites with different isotopes and metal ions.[3,7-10] The sequential ferric binding constants are $10^{20.7}$ and $10^{19.4}$ at pH 7.4 and atmospheric pCO_2.[11] With this great affinity of transferrin for Fe^{3+} it is no surprise that ligand exchange is usually slow.[5,12,13] The detailed chemical process by which iron is removed from the protein is unknown, although the biological processes involved in recognition of the protein, its incorporation into a vesicle within the cell, iron release at low pH in an endosome, and release of the protein from the cell by endocytosis, are all characterized.[14]

The question of the chemical process by which iron is removed from transferrin is especially relevant to the treatment of toxic iron overload. Certain blood disorders such as sickle cell anemia and β-thalassemia require frequent whole blood transfusions.[15] Because of the lack of a human physiological mechanism to excrete iron, this therapy can lead to the accumulation of iron in tissues and organs. Desferrioxamine B, the current drug of choice, is thermodynamically capable of removing iron from transferrin; however, it is kinetically slow.[16] More effective chelating agents are being sought to remove iron from transferrin before deposition.[15,17] To date, the fastest known ligands are synthetic catecholates modeled after the catecholate siderophore enterobactin.[13,18]

Our studies probe the elucidation of the mechanism and kinetic barriers for iron delivery to and from transferrin. Several mechanisms have been proposed for iron removal from transferrin. One suggested by Carrano and Raymond[13] predicts the formation of a ternary species involving Fe^{3+}, transferrin, and the competing ligand:

$$\mathrm{FeTf} + \mathrm{L} \underset{k_2}{\overset{k_1}{\rightleftharpoons}} \mathrm{FeTfL} \xrightarrow{k_3} \mathrm{FeL} + \mathrm{Tf} \qquad (1)$$

where Tf = bicarbonate complex of transferrin and L = hexadentate ligand.

The exact solutions of these rate equations are complex two-term exponentials that will not be discussed in this paper.[19,20] For the observed rate described as

$$d[\mathrm{FeL}]/dt = k_{obsd}[\mathrm{FeTf}] \qquad (2)$$

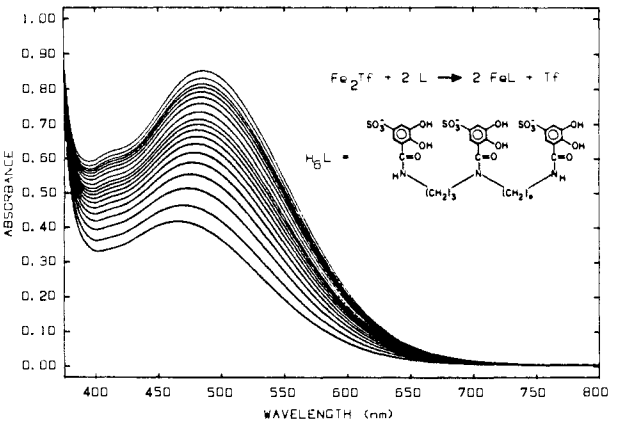

Figure 1. Absorbance spectra for the reaction of 0.100 mM diferric-transferrin (Fe_2Tf) and 6.00 mM 3,4-LICAMS (L) (0.050 M HEPES, pH 7.4, 25 °C, μ = 0.082). The absorbance increases and λ_{max} shifts to 495 nm as ferric 3,4-LICAMS (FeL) is formed. The schematic reaction does not include the proton stoichiometry. H_6L = *N,N',N''*-tris(5-sulfo-2,3-dihydroxybenzoyl)-1,5,10-triazadecane (3,4-LICAMS).

(where [FeTf] will represent the concentration of the ferric transferrin *plus* any FeTfL intermediate), simple equations result from the assumed relative values for the rate constants.

(A) If the FeTfL kinetic intermediate grows to be large with respect to the ferric transferrin, saturation of the rate with increasing ligand concentration will occur. This can be seen from the improved steady-state approximation:[21]

$$k_{obsd} = \frac{k_1 k_3[\mathrm{L}]}{k_1[\mathrm{L}] + k_2 + k_3} \qquad (3)$$

(B) If the intermediate is the major iron-containing species early in the reaction and formed in an essentially pre-equilibrium step, k_3 is small compared to k_2 and the observed rate constant becomes[21]

$$k_{obsd} = \frac{k_1 k_3[\mathrm{L}]}{k_1[\mathrm{L}] + k_2} \qquad (4)$$

For either case, at sufficiently high ligand concentrations the stoichiometric constants make the observed rate become independent of ligand concentration and equivalent to k_3. A hyperbolic relationship between the observed rate constant for iron removal from diferric transferrin and the concentration of chelating ligand is expected from (4) and was earlier interpreted as supporting model B,[13] although there was no independent evidence for the ternary complex.

Cowart, Kojima, and Bates have proposed an alternate mechanism for iron *delivery* to transferrin by acetohydroxamic acid which involves a ternary transferrin/iron/ligand intermediate, and evidence for this intermediate in iron delivery to the protein was shown.[22] However, no intermediate was observed when iron was removed from diferric transferrin with excess acetohydroxamic acid. To explain these observations, a mechanism was proposed which involves a unimolecular conformational change of the protein as the last step of the mechanism.[22] If the stable form of diferric transferrin is a conformation in which the metals are buried within the protein (and so protected against attack by chelators), then that protein must undergo a change to an open conformation in which the metal sites are exposed to the solution environment before metal exchange can occur.

Applying the principle of microscopic reversibility to the Cowart, Kojima, and Bates mechanism[22] shows how iron would then be removed from the transferrin by a chelating agent:

(2) Aisen, P.; Listowsky, I. *Annu. Rev. Biochem.* **1980**, *49*, 357–393.
(3) Chasteen, N. D. *Coord. Chem. Rev.* **1977**, *22*, 1–36.
(4) Feency, R. E.; Komatsu, S. K. *Struct. Bonding (Berlin)* **1969**, *1*, 148–206.
(5) Harris, W. R. *J. Inorg. Biochem.* **1984**, *21*, 263–276.
(6) Chasteen, N. D.; White, L. K.; Campbell, R. F. *Biochemistry* **1977**, *16*, 363–368.
(7) Cannon, J. C.; Chasteen, N. D. *Biochemistry* **1975**, *14*, 4573–4577.
(8) Princiotto, J. V.; Zapolski, E. J. *Nature (London)* **1975**, *255*, 87–88.
(9) Harris, D. C. *Biochemistry* **1977**, *16*, 560–564.
(10) Baldwin, D.; de Sousa, D. M. *Biochem. Biophys. Res. Commun.* **1981**, *99*, 1101–1107.
(11) Aisen, P.; Leibman, A.; Zweier, J. *J. Biol. Chem.* **1978**, *253*, 1930–1937.
(12) Baldwin, D. *Biochim. Biophys. Acta* **1980**, *623*, 183–198.
(13) Carrano, C. J.; Raymond, K. N. *J. Am. Chem. Soc.* **1979**, *101*, 5401–5404.
(14) Klausner, R. D.; Rao, K.; Roualt, T.; Weissman, A.; Marford, J. *Abstracts, VIIth International Conference on Proteins of Iron Metabolism*; Lille, France, 1985; p 14.
(15) Martell, A. E., Anderson, W. F., Badman, D. G., Eds. *Development of Iron Chelators for Clinical Use*; Elsvier/North-Holland: New York; 1981.
(16) Pollack, S.; Vanderhoff, G.; Lasky, F. *Biochim. Biophys. Acta* **1977**, *497*, 481–484.
(17) Anerson, W. F., Hiller, M. C., Eds. *Proceedings of a Symposium on Development of Iron Chelators for Clinical Use*; DHEW: Washington, DC, 1975; DHEW Publication No. (NIH) 77-994.
(18) Rodgers, S. J.; Raymond, K. N. *J. Med. Chem.* **1983**, *26*, 439–442.
(19) McDaniel, D. H.; Smoot, C. R. *J. Phys. Chem.* **1956**, *60*, 966–969.
(20) Frost, A. A.; Pearson, R. G. *Kinetics and Mechanisms*, 3rd ed., Wiley: New York, 1961; pp 160–199.
(21) Strickland, S.; Palmer, G.; Massey, V. *J. Biol. Chem.* **1975**, *250*, 4048–4052.
(22) Cowart, R. E.; Kojima, N.; Bates, G. W. *J. Biol. Chem.* **1982**, *257*, 7560–7565.

$$\mathrm{FeTf} \underset{k_{-1}}{\overset{k_1}{\rightleftharpoons}} \mathrm{FeTF^*} \qquad (5)$$

$$\mathrm{FeTf^* + L} \underset{k_{-2}}{\overset{k_2}{\rightleftharpoons}} \mathrm{FeTfL^*}$$

$$\mathrm{LFeTF^*} \xrightarrow{k_3} \mathrm{FeL + Tf^*}$$

$$k_{obsd} = \frac{k_1 k_2 k_3[\mathrm{L}]}{k_{-1}(k_{-2} + k_3) + k_2 k_3[\mathrm{L}]}$$

where * = "open conformation", Tf = bicarbonate complex of transferrin, and L = hexadentate ligand. When excess ligand is used, the observed rate becomes first order, since the first step is then rate-determining. According to this mechanism, iron may be removed no faster than the rate at which diferric transferrin transforms to its open form.

With EDTA as an iron removal agent, Baldwin et al. have explored the iron removal mechanism from ferric transferrin, using EDTA concentrations as high as 0.3 M because EDTA is a poor iron chelating agent relative to transferrin.[10,12,22] It seemed likely to us that this may have affected the protein, since anion binding significantly influences the rates of iron removal from the two sites.[1,10] In our experiments, we have used *N,N',N''*-tris(5-sulfo-2,3-dihydroxybenzoyl)-1,5,10-triazadecane (3,4-LICAMS, see Figure 1) as the chelating ligand. The advantage of using 3,4-LICAMS is that its fast rates of iron removal allow the concentration of ligand to be reduced by an order of 100, thereby decreasing the chance of ligand allosteric effects.

Baldwin reported biphasic kinetics of iron removal from transferrin by EDTA, which he interpreted as due to kinetic heterogeneity of the N-terminal and C-terminal sites, and he proposed a two-path kinetic model which reflected this.[12] Our data support the model of kinetic inequivalence between the two sites: iron is removed by 3,4-LICAMS from the N-terminal site at faster rates than from the C-terminal site at 25 °C. Activation enthalpies, determined from the temperature dependence of iron removal from the monoferric transferrins, further support our findings: at higher temperature the activation enthalpy for iron removal from the N-terminal site is lower than that from the C-terminal site. A break in linearity in the Arrhenius plot for iron removal from the N-terminal monoferric transferrin is interpreted as an indication that the N-terminal site undergoes a conformational change near 20 °C which changes the rate of iron mobilization from the site.

Experimental Section

Distilled deionized water was used at all times unless otherwise indicated. Glassware was washed with phosphate-free RBS-pf (Pierce Chemical Co.) and rinsed thoroughly with tap distilled water. Dialysis tubing (Bethesda Research Laboratories) was boiled in water, stored in a solution containing 0.1% EDTA and 0.02% NaN_3, and washed several times with water prior to use. All solutions were adjusted to pH 7.40 at 25 °C unless otherwise indicated. Urea–polyacrylamide gel electrophoresis was carried out by using standard procedures.[23,24]

Diferric Transferrin. Human serum apotransferrin (Sigma Chemical Corporation or Calbiochem-Behring) was dissolved in water (20 mg/mL) and dialyzed at 4 °C for a minimum of 9 h against several changes of water and then against a solution containing 0.050 M *N*-(2-hydroxyethyl)piperazine-*N'*-2-ethanesulfonic acid buffer (HEPES) and 0.001 M $NaHCO_3$ to remove chelate contaminants.[25,26] The protein was saturated to 97% of total sites by addition of freshly prepared 0.002 M ferric nitrilotriacetate [$Fe(NTA)_2$] (Eastman Chemical Corporation).[26] [To avoid hydrolysis of the $Fe(NTA)_2$, NTA was dissolved in water at pH 4.0, ferric chloride at pH 1.0 was added, and the pH was brought to 4.0 with dilute NaOH.] After 2 h, the resulting red complex was dialyzed at 4 °C for a minimum of 20 h against several changes of a solution containing 0.1 M $NaClO_4$ and 0.050 M HEPES to remove NTA and excess iron and $NaHCO_3$. The desired buffer was used as the final dialysite. The extinction coefficients used were 9.23×10^4 M^{-1} cm^{-1} at λ_{max} 279 nm and 2500 M^{-1} cm^{-1} at λ 466 nm.[13,25]

Diferric transferrin was also prepared by adding enough $Fe(NTA)_2$ to C-terminal monoferric transferrin in a solution containing 0.010 M $NaHCO_3$, 0.050 M HEPES, and 0.1 M $NaClO_4$ to saturate 50% of the sites. This was stirred and dialyzed at 4 °C against several changes of a solution containing 0.050 M HEPES and 0.1 M $NaClO_4$ and finally against 0.050 M HEPES.

C-Terminal Monoferric Transferrin. Apotransferrin was dissolved and dialyzed as described above. Freshly prepared $Fe(NTA)_2$ was added to the apotransferrin at pH 7.40 to saturate 50% of the sites. The solution immediately turned red and was stirred for 5 min at room temperature. It was dialyzed against a 0.1 M $NaClO_4$ and 0.050 M HEPES solution for 3 h at 25 °C and for 12 h at 4 °C and finally against 0.050 M HEPES adjusted to pH 7.40 at the desired temperature. Urea–polyacrylamide gel electrophoresis was then used to verify the purity of the C-terminal monoferric transferrin.

N-Terminal Monoferric Transferrin.[27] Apotransferrin was dialyzed at 4 °C against several changes of water and finally against a solution of 0.050 M HEPES and 0.02 M $NaHCO_3$, pH 7.80. Freshly prepared $Fe(NTA)_2$ at pH 4.0 was added to saturate 100% of the sites. The red solution was left overnight at room temperature and then diluted to 0.02 mM with a solution in which the final concentration of species were 0.1 M HEPES, 1 M $NaClO_4$, and 1 mM pyrophosphate, pH 7.5. Desferrioxamine B (CIBA Pharmaceutical Co.) was added as a solution to give a final concentration of 1 mM. The solution was left to stand for 4 h at room temperature. Under these conditions, iron was preferentially removed from the C-terminal site as was confirmed by electrophoresis. The solution was dialyzed at 4 °C against several changes of 0.050 M HEPES which had been filtered on Bio-Rad Chelex 100 (100–200 mesh, Na^+). The protein was concentrated by ultrafiltration (Amicon PM-10 membrane) while stirring under N_2 at 4 °C. The N-terminal monoferric transferrin needed for temperature studies was dialyzed against 0.050 M HEPES adjusted to pH 7.40 at the appropriate temperature.

Radioactive Isotope Labeled Transferrin. A solution of $Fe(NTA)_2$ was prepared with a 7% excess of NTA. Either $^{55}FeCl_3$ or $^{59}FeCl_3$ in 0.5 M HCl (New England Nuclear) was added to give an ^{55}Fe:Fe ratio of $\sim 5 \times 10^{-4}$ and an ^{59}Fe:Fe ratio of $\sim 5 \times 10^{-6}$, where the total concentration of Fe per site was 0.05 mM. The pH was raised to 4.0 with 1 equiv of 0.5 M NaOH. The C-terminal site was labeled by using the labeled $Fe(NTA)_2$ to make C-terminal monoferric transferrin and then unlabeled $Fe(NTA)_2$ to fill the N-terminal sites as previously described. The N-terminal site was labeled by adding labeled $Fe(NTA)_2$ to C-terminal monoferric transferrin.

Visible Spectroscopy. Kinetic studies of iron removal from monoferric and diferric transferrins by 0.40–12.00 mM *N,N',N''*-tris(5-sulfo-2,3-dihydroxybenzoyl)-1,5,10-triazadecane (3,4-LICAMS)[28,29] were performed in 1-cm quartz cuvettes maintained at constant temperature and monitored at 520 nm by visible spectroscopy using a Hewlett-Packard 8450A spectrophotometer equipped with a thermostated cell. Solutions containing 0.050–0.100 mM filtered iron transferrin (0.2-μm Gelman Acrodiscs) in the desired buffer were prepared. Potassium chloride was used as the supporting electrolyte for maintaining constant ionic strength. The reference cell contained appropriate amounts of ligand, buffer, and KCl.

The time of mixing protein with ligand was recorded as zero time and scans were obtained every 2–15 min depending on the reaction rate (approximately 10 scans per half-life were desired). Absorbance values vs. wavelength or time were collected and stored on double-density two-sided floppy disks.

Scintillation Counting. Labeled diferric transferrin and 6 mM 3,4-LICAMS were mixed together in a scintillation vial. Potassium chloride was used to adjust the ionic strength. Aliquots of 0.200 mL were taken at 3–5-min intervals for 65 min and 5–10-min intervals for the following 70 min. These were immediately passed down Bio-Rad AG-1-X4 (100–200 mesh, Cl^-) anion exchange columns (0.5 × 4 cm) equilibrated with 0.050 M HEPES. The columns were washed with 2 mL of buffer and the elutants were collected in screw-capped vials. This allowed for separation of apo, monoferric, and diferric transferrins from ferric 3,4-LICAMS since the 3,4-LICAMS adhered strongly to the columns. Next, 0.200 mL of each elutant was placed in scintillation vials along with 10 mL of Aquasol (Du Pont). The vials were capped, shaken, and placed in the Mark III liquid scintillation system Model 6880 where counts per minute were measured. These were converted to decays per minute by a variable quench mode which used previously determined calibration curves.[30]

(23) Chasteen, N. D.; Williams, J. *Biochem. J.* **1981**, *193*, 717–727.
(24) Makey, D. G.; Seal, U. S. *Biochim. Biophys. Acta* **1976**, *453*, 250–256.
(25) Bates, G. W.; Schlabach, M. R. *J. Biol. Chem.* **1973**, *248*, 3228–3232.
(26) Bates, G. W.; Wernicke, J. *J. Biol. Chem.* **1971**, *246*, 3679–3685.
(27) Chasteen, N. D., private communication, March 21, 1985.
(28) Weitl, F. L.; Harris, W. R.; Raymond, K. N. *J. Med. Chem.* **1979**, *22*, 1281–1283.
(29) Raymond, K. N.; Muller, G.; Matzanke, B. F. *Top. Curr. Chem.* **1984**, *123*, 49–102.

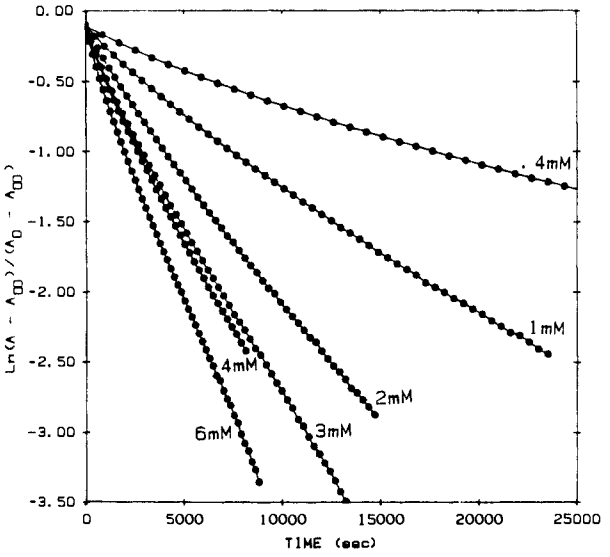

Figure 2. Iron removal from 0.100 mM diferric transferrin by various concentrations of 3,4-LICAMS (0.050 M HEPES, pH 7.4, 25 °C, μ = 0.082).

Results and Discussion

Kinetics of Iron Removal from Diferric Transferrin. Addition of 3,4-LICAMS to a solution of diferric transferrin in 0.050 M HEPES buffer resulted in a shift of the band maximum at 466 nm of the diferric transferrin to a band maximum at 495 nm, characteristic of tris(catecholato)iron(III) complexes. Figure 1 shows the observed spectral changes which indicate that iron was being removed from diferric transferrin by 3,4-LICAMS.

In order to calculate rates of Fe removal, the kinetics were monitored at 520 nm. The concentrations of ligand used for our analyses were in 10–30-fold excess over total iron sites in diferric transferrin. For direct comparison with the previous study,[13] concentrations of ligand ranging from 2- to 30-fold excess over total iron sites in diferric transferrin were used. Plots of ln $[(A - A_\infty)/(A_0 - A_\infty)]$ vs. time are shown in Figure 2. These do not conform to the linear behavior reported by Carrano and Raymond.[13] Similar results were obtained when the experiment was repeated in the tris(hydroxymethyl)aminomethane (TRIS) buffer system as described by Carrano. We speculate from reconstruction of the previous experiments that the observed first-order behavior was due to discarding the first few absorbance values (about 10% of the iron removal) in the kinetic runs with the belief that nonspecifically bound iron might be involved in this phase of iron release from transferrin. However, nonspecifically bound iron is removed by perchlorate treatment of the protein;[25] we observed no change in kinetic behavior for transferrin that had been overloaded by 50% with Fe^{3+} prior to the perchlorate treatment.

Several possible causes for the deviations from linearity in the first-order plots were investigated. Preparations of protein and $Fe(NTA)_2$ solutions were found satisfactory by gel electrophoresis and spectrophotometric titrations, respectively. Complete characterization of the ligand purity by HPLC and FAB mass spectroscopy eliminated ligand artifacts as a cause. Although salts are known to affect the kinetics of Fe removal from the two sites of transferrin,[10] curvature arising from the addition of KCl to correct for ionic strength differences between 0.050 M HEPES and 0.100 M TRIS and the various concentrations of 3,4-LICAMS is unlikely since the concentration of KCl was only 0.061 mM, and no significant effects were observed in controls containing 0–0.2 mM KCl. Ligand oxidation caused slight drifts in the A_∞ values.[31] However, distortion of the estimated A_∞ values was avoided by nonlinear-least-squares refinement. Also, first-order plots using the Guggenheim method,[32] which does not require the knowledge of A_∞, were nonlinear.

Nonlinear first-order kinetic behavior has been reported by Baldwin for iron removal from diferric transferrin by EDTA. He proposed the following scheme for irreversible iron release:[12]

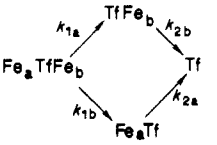

Baldwin solved the simultaneous rate equations.[12] (An alternative, linear algebraic derivation is shown below.)[33] Assuming that the extinction coefficient is the same in both sites and the absorbance due to apotransferrin at 466 and 520 nm is zero, the following relationship between change in absorbance and time is obtained (we have adapted Baldwin's notation):[12]

$$A - A_\infty = B_0 \epsilon l \left[\left(2 - \frac{k_{1a}}{m_1 - m_2} - \frac{k_{1b}}{m_1 - m_3} \right) e^{-m_1 t} + \frac{k_{1a}}{m_1 - m_2} e^{-m_2 t} + \frac{k_{1b}}{m_1 - m_3} e^{-m_3 t} \right] \quad (6)$$

where B_0 = concentration of diferric transferrin at initial time, ϵ = molar extinction coefficient per iron, l = cell path length, $m_1 = k_{1a} + k_{1b}$, $m_2 = k_{2b}$, and $m_3 = k_{2a}$.

When the two sites are similar but not identical, the equation can be further simplified:

$$m_1 > m_2 \approx m_3$$

$$A - A_\infty = B_0 \epsilon l \left[\left(2 - \frac{m_1}{m_1 - m_2} \right) e^{-m_1 t} + \frac{m_1}{m_1 - m_2} e^{-m_2 t} \right] \quad (7)$$

This predicts biphasic release expressed in terms of two macroscopic rate constants, m_1 and m_2, with an apparent percentage of iron released in the faster initial phase of

$$50\left(2 - \frac{m_1}{m_1 - m_2} \right)\% \quad (8)$$

As seen from this equation, only when $m_1 >> m_2$ does the percentage of each phase approach 50%. A third assumption, that the two sites are noncooperative,[1,5] further simplifies the model by equating k_{1a} with k_{2a} and k_{1b} with k_{2b}, thereby reducing the total number of rate constants to two microscopic rate constants, k_{1a} and k_{1b}.

Our data were analyzed using nonlinear-least-squares programs, ORGLS and MARQFIT.BAS, with eq 7.[34,35] The parameters refined were A_0, A_∞, m_1, and m_2. The observed rate constants are shown

Table I. Macroscopic Rate Constants for Iron Removal from 0.100 mM Diferric Transferrin by 3,4-LICAMS[f]

[3,4-LICAMS], mM	m_1[a] × 10^2, min^{-1}	m_2[b] × 10^2, min^{-1}	% m_1[c]	k_{obsd}[d] × 10^2, min^{-1}
6.00	7.0 (1)[e]	1.95 (2)	36 (1)	2.1
4.00	5.2 (1)	1.48 (8)	36 (1)	1.8
3.00	4.7 (1)	1.38 (2)	35 (1)	1.3
2.00	3.36 (8)	1.02 (4)	35 (1)	1.1
1.00	1.91 (6)	0.52 (4)	36 (2)	0.63
0.40	0.9 (1)	0.19 (8)	40 (8)	0.30

[a] $m_1 = k_{1a} + k_{1b}$. [b] $m_2 = k_{2b}$. [c] Calculated from eq 8. [d] From ref 13 (0.1 M TRIS, pH 7.4, 25 °C, μ = 0.082). [e] See ref 37. [f] 0.050 M HEPES, pH 7.4, 25 °C, μ = 0.082.

(30) Manual for Mark III Liquid Scintillation System, Model 6880; Searle Analytic Inc., 1975.

(31) Avdeef, A.; Sofen, S. R.; Bregante, T. L.; Raymond, K. N. *J. Am. Chem. Soc.* **1978**, *100*, 5363–5370.

(32) Fleck, G. M. *Chemical Reaction Mechanisms*; Holt, Reinhardt, and Winston: San Francisco, 1971; pp 37–44.

(33) A linear algebraic approach can be used to simplify the integration of the differential equations (see Appendix).

(34) Busing, W. R.; Levy, H. A. ORGLS, *A General FORTRAN Least Squares Program*; Oak Ridge National Laboratory: Oak Ridge, TN, 1962; publication ORNL-TM-271. This program uses a Taylor-series (Gauss–Newton) method to find a minimum.

(35) Schreiner, W.; Kramer, M.; Krisher, S.; Langsam, Y. *PC Tech J.* **1985**, *3*, 170–199. This program uses a gradient (steepest descent) method followed by the Gauss–Newton method to find a minimum.

Table II. Rate Constants for Iron Removal from 0.100 mM Labeled Diferric Transferrin by 6 mM 3,4-LICAMS[g]

	N-labeled site		C-labeled site	
	55Fe(N)-Fe(C)Tf ×10², min⁻¹	59Fe(N)-Fe(C)Tf × 10², min⁻¹	55Fe(C)-Fe(N)Tf × 10², min⁻¹	59Fe(C)-Fe(N)Tf ×10², min⁻¹
Fe(total)[a]				
m_1[b]	6.9 (2)	7.0 (2)	6.3 (1)	6.3 (1)
m_2[c]	2.35 (6)	1.94 (6)	1.79 (4)	1.93 (2)
% m_1[d]	33 (2)	36 (2)	36 (1)	35 (1)
k_{1a}[Fe(N)][e]	3.2 (2)	3.1 (5)	4.7 (7)	4.8 (6)
k_{1b}[Fe(C)][f]	2.2 (3)	2.0 (2)	1.4 (2)	1.4 (2)
m_1[Fe(N) + Fe(C)]	5.4 (3)	5.1 (5)	6.0 (7)	6.2 (6)
m_1[Fe(total)]/ m_1[Fe(N) + Fe(C)]	1.3 (1)	1.4 (1)	1.0 (1)	1.0 (1)

[a] Fe(total) refers to the total amount of iron in diferric transferrin. [b] $m_1 = k_{1a} + k_{1b}$. [c] $m_2 = k_{2b}$. [d] Calculated from eq 8. [e] Fe(N) refers to the iron located in the N-terminal site of diferric transferrin. [f] Fe(C) refers to the iron located in the C-terminal site of diferric transferrin. [g] 0.050 M HEPES, pH 7.4, 25 °C, μ = 0.082.

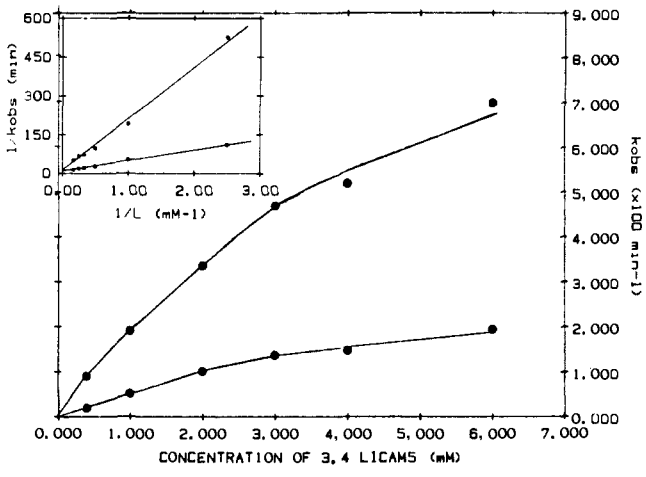

Figure 3. Plot of observed rate constants as a function of increasing concentrations of 3,4-LICAMS as determined by nonlinear least-squares analyses for iron removal from 0.100 mM diferric transferrin (0.050 M HEPES, pH 7.4, 25 °C, μ = 0.082). The macroscopic rate constants m_1 and m_2 give rise to the upper and lower curves, respectively. The inset shows the linear reciprocal plots of the two curves. The label for the x axis, $1/L$, is equivalent to the reciprocal of the ligand concentration.

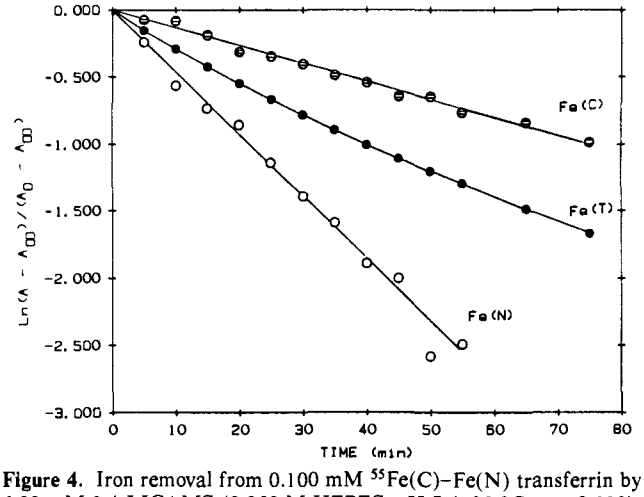

Figure 4. Iron removal from 0.100 mM ^{55}Fe(C)-Fe(N) transferrin by 6.00 mM 3,4-LICAMS (0.050 M HEPES, pH 7.4, 25 °C, μ = 0.082). The filled circles represent the total iron removed [Fe(T)], the striped circles represent iron removed from the C-terminal site [Fe(C)], and the empty circles represent iron removed from the N-terminal site [Fe(N)]. The data have been normalized in order to fit all on the same plot.

in Table I along with the percentages of iron released during the first phase (% m_1) for several different concentrations of 3,4-LICAMS. The calculated values of A_0 and A_∞ were identical with those obtained directly from the visible spectra. The observed macroscopic rate constants are plotted against ligand concentration in Figure 3. It appears that the rates of iron removal of the first phase were 4–5 times faster than the corresponding rates of the second phase, 35–40% of the iron was released during the first phase, and the latter phase was similar to that reported by Carrano. Finally, both phases reached saturation in accordance with the Cowart–Bates or Carrano–Raymond mechanisms discussed previously.

Kinetics of Fe Removal from Isotopically Labeled Transferrin. Because the macroscopic rate constant m_1 is the sum of k_{1a} and k_{1b}, separate values for the two microscopic rate constants cannot be obtained from the previously described experiment. Since iron is not exchanged between the two binding sites, it is possible to specifically label one site with radioactive iron.[9,36] Thus we can independently monitor the kinetics of iron removal from the two sites. Again, assuming that the two sites are noncooperative, the four microscopic rate constants can be reduced to two, corresponding to the rates of iron removal from the two individual sites.

The rate of iron released from the isotopically labeled site was monitored by scintillation counting. At timed intervals, samples from the initial reaction mixtures were placed directly onto Bio-Rad AG-1-X4 (100–200 mesh, Cl^-) anion exchange resin columns equilibrated with 0.050 M HEPES buffer at pH 7.4, 25 °C. This served to quench the reaction and separate the ferric transferrin from the ferric 3,4-LICAMS, because the former was eluted with the buffer solution while the highly charged ferric 3,4-LICAMS remained fixed on the column. The amount of radioactive iron removed from transferrin was obtained by scintillation counting of the elutants and used to determine the rate of iron removal from the labeled site. Simultaneous monitoring of the rate of total iron released from diferric transferrin using visible spectroscopic methods allowed for calculation of the rate of iron released from the nonlabeled site by subtraction of the millimoles of iron remaining in the labeled site from the total millimoles of iron remaining. Figure 4 shows the results for a typical experiment in which the C-terminal site was labeled with ^{55}Fe. The data have been normalized in order to plot all results on the same graph. Plots of iron removal from the two individual sites were linear and were analyzed using linear-least-squares regression while those of the total iron were curved as shown previously in Figure 3 and were analyzed as described using eq 7. A summary of four separate experiments is given in Table II.

From these results it is apparent that iron was removed from the N-terminal site at higher rates than from the C-terminal site under the experimental conditions described. Iron removal from each individual site appeared to be a first-order process, while the combined process was biphasic. Assuming no cooperativity, this determines k_{1a} and k_{1b} (and k_{2a} and k_{2b}). According to the Baldwin model, the sum of k_{1a} and k_{1b} should yield m_1 and k_{1b} should equal m_2. When the "b" site was equated to the C-terminal site, this seemed to hold true as shown in Table II. The closest fit to the Baldwin model was found for the data obtained from the experiments in which the C-terminal site was labeled with the radioactive iron isotopes, as might be expected, since the accuracy of the scintillation counting measurements was increased in this

(36) Fletcher, J.; Huehns, E. R. *Nature (London)* **1967**, *215*, 584–586.

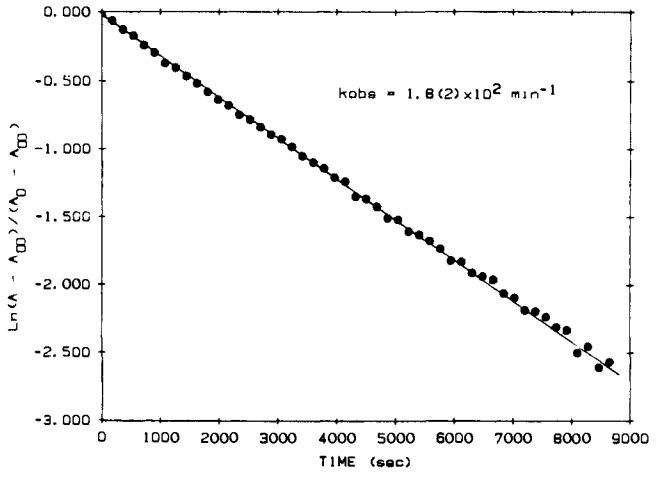

Figure 5. Iron removal from 0.100 mM C-terminal monoferric transferrin by 6.00 mM 3,4-LICAMS (0.050 M HEPES, pH 7.4, 25 °C, μ = 0.082).

case due to the slower rate of Fe removal from this site. The percentages of Fe removed in the first phase were calculated by using eq 8 with the macroscopic rate constants found from the nonlinear-least-squares analyses.

Kinetics of Iron Release from the Monoferric Transferrins. The kinetics of iron removal from C-terminal monoferric transferrin by 6 mM 3,4-LICAMS were monitored as described for the diferric transferrin. First-order plots of ln $[(A - A_\infty)/(A_0 - A_\infty)]$ vs. time were linear as expected, since the iron was located in only one site (see Figure 5). The average rate constant found was 1.8 (2) $\times 10^{-2}$ min^{-1}.[37] This agrees with the macroscopic and microscopic rate constants, m_2 and k_{1b}, found earlier for diferric transferrin.

Similarly, the removal of iron from N-terminal monoferric transferrin by 6 mM 3,4-LICAMS was found to be a first-order process with an average rate of 2.3 (5) $\times 10^{-2}$ min^{-1}. This is slightly less than the values found in the isotope labeling experiment. Nonetheless, we can conclude that iron was removed from the N-terminal site at a slightly faster rate than from the C-terminal site under the conditions of this experiment.

Curvature of the rate with time was often observed during the very early stages (less than 10% of the total reaction) of the monoferric transferrin first-order plots, with the remainder of the reaction exactly linear. We have attributed this to the presence of small amounts of other ferric transferrins. This was confirmed by urea–polyacrylamide gel electrophoresis. Attempts to refine these data using the biphasic model described earlier were unsuccessful.

If cooperactivity between the two sites exists, then derived rate constants 2.3 (5) $\times 10^{-2}$ and 1.8 (2) $\times 10^{-2}$ min^{-1} correlate to k_{2a} and k_{2b}, respectively, of the Baldwin model. These values were fixed in Baldwin's exact solution (eq 6), and k_{1a} and k_{1b} were found by the MARQFIT.BAS program.[35] The microscopic rate constant, k_{1b} [1.9 (4) $\times 10^{-2}$ min^{-1}], agreed well with k_{2b} [1.8 (2) $\times 10^{-2}$ min^{-1}] while k_{1a} [4.8 (4) $\times 10^{-2}$ min^{-1}] was greater than k_{2a} [2.3 (5) $\times 10^{-2}$ min^{-1}]. Possibly, the noncooperative assumption, at least for the N-terminal site, is not correct. This may explain the higher rate constants found for iron removal from radioactively labeled diferric transferrin (see Table II). In fact, the latter values were closer to the average of k_{1a} and k_{2a} (3.6 $\times 10^{-2}$ min^{-1}). In any case, k_{1a} and k_{2a} were both greater than k_{1b} and k_{2b}, indicating that iron was more readily removed from the N-terminal site under the described experimental conditions.

Temperature Dependence. The temperature dependence of the kinetics of iron removal from the two monoferric transferrins by 3,4-LICAMS was examined to determine the effective activation enthalpies. A high concentration of 3,4-LICAMS was used to ensure that the observed rate constants had reached the saturation level with respect to ligand concentration at each temperature ranging from 4 to 37 °C. Ionic strength and pH were kept constant. As shown in Figure 6, a linear relationship between ln k and $1/T$ was obtained for iron removal from C-terminal monoferric transferrin, the slope of which yielded an activation enthalpy of 20 (1) kcal/mol. However, two distinctly different linear regions were observed for iron removal from the N-terminal site. Repetition of this experiment gave identical results with an obvious break occurring between 12 and 20 °C. The activation enthalpies found were 21 (2) kcal/mol for temperatures below 20 °C and 15 (1) kcal/mol for temperatures above 20 °C. The higher activation enthalpy for the removal of iron from the C-terminal monoferric transferrin at 25 °C parallels the slower observed rates. Table III lists the rates of iron removal from the two monoferric transferrins at various temperatures. Notice that the rates were similar at the lower temperatures, where the activation enthalpies were approximately equivalent. At the higher temperatures, iron was removed at much faster rates from the N-terminal site.

The break in the Arrhenius plot and the lowered activation energy for N-terminal monoferric transferrin may result from a temperature-induced conformational change. As there are three more disulfide linkages in the C-terminal site, which confer greater conformational stability,[38] we might expect that the N-terminal

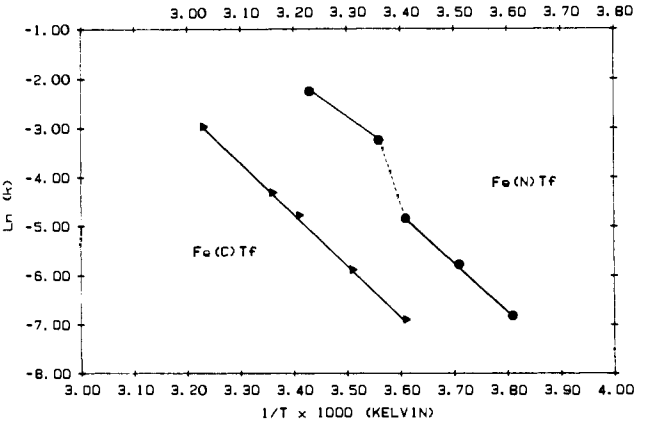

Figure 6. Plot of observed rate constants as a function of temperature for iron removal from 0.09 mM C- and N-terminal monoferric transferrins [Fe(C)Tf and Fe(N)Tf, respectively] by 12.00 mM 3,4-LICAMS (0.050 M HEPES, pH 7.4, μ = 0.175). The lower scale corresponds to the plot of the data from Fe(C)Tf, and the upper scale, which has been offset by 0.2 K, corresponds to the plot of the data from Fe(N)Tf. (See text regarding the reproducibility of the experiment.)

Table III. Rate Constants and Activation Enthalpies for Iron Removal from 0.09 mM Monoferric Transferrins by 12 mM 3,4-LICAMS[e]

temp, °C	Fe(C)Tf,[a] $k_{obsd} \times 10^2$, min^{-1}	Fe(N)Tf,[b] $k_{obsd} \times 10^2$, min^{-1}	k_{obsd}[Fe(N)Tf]/ k_{obsd}[Fe(C)Tf]
4	0.101 (1)	0.109 (2)	1.08
12	0.279 (2)	0.31 (1)	1.1
20	0.85 (2)	0.79 (3)	0.93
25	1.35 (2)	3.9 (2)	2.9
37	5.2 (1)	10.6 (4)	2.0
	$\Delta H^\ddagger$		
	Fe(C)Tf, kcal mol^{-1}	Fe(N)Tf, kcal mol^{-1}	$\Delta H^\ddagger$[Fe(N)Tf]/ $\Delta H^\ddagger$[Fe(C)Tf]
low temp[c]	20 (1)	21 (2)	1.0
high temp[d]	20 (1)	15 (1)	0.75

[a] Fe(C)Tf = C-terminal monoferric transferrin. [b] Fe(N)Tf = N-terminal monoferric transferrin. [c] Temperatures ranging from 4 to 12 °C. [d] Temperatures ranging from 20 to 37 °C. [e] 0.050 M HEPES, pH 7.4, 25 °C, μ = 0.175.

(37) This is equivalent to (1.8 ± 0.2) $\times 10^{-2}$ min^{-1}. Here and elsewhere, the estimated standard deviation (in the least significant digits) is presented in parentheses following the corresponding parameter.

(38) MacGillivray, R. T.; Mendez, E.; Sinha, S. K.; Sutton, M. R.; Lineback-Zins, J.; Brew, K. *Proc. Natl. Acad. Sci. U.S.A.* **1982**, *79*, 2504–2508.

site undergoes a conformational change more readily than the C-terminal site. Further evidence for such a change can be seen by examination of the percentages of released iron associated with each phase of iron removal from diferric transferrin at 25 °C. The fact that this stayed constant as the concentration of ligand was increased signifies that any major conformational change has been completed at these conditions.

It should be noted that Binford and Foster measured the enthalpy change at 25 °C, pH 7.96, for the reaction of $Fe(NTA)_2$ with apotransferrin by direct calorimetry.[39] The enthalpy changes for saturation of half of the binding sites and saturation of the half-saturated protein were ≃10.90 (19) and −10.43 (76) kcal/mol of bound Fe, respectively. The identical values suggest that the sites are similar; however, these results cannot be correlated with enthalpy changes for loading of the individual sites and, hence, cannot be compared with the activation enthalpies reported here.

Conclusions

These results demonstrate that iron is removed at a faster rate from the N-terminal site of transferrin at pH 7.4 and temperatures above 20 °C with 3,4-LICAMS than from the C-terminal site. One interpretation is that the less rigid N-terminal site undergoes a conformational change at 20 °C which facilitates the removal of iron and lowers the activation enthalpy for the process at physiological temperatures relative to the C-terminal site. The biphasic kinetic behavior of iron removal from diferric transferrin supports the Baldwin model, which recognizes the kinetic inequivalence of the two sites.

The observed rates of the two phases of iron removal from diferric transferrin reach saturation with respect to ligand concentration as predicted by both the Carrano–Raymond and Cowart–Bates mechanisms. Additional studies are in progress to distinguish between them. Whatever the mechanism, it appears that the kinetic inequivalence of the two sites of transferrin is a general phenomenon for iron removal by powerful chelating agents.

Acknowledgment. This research is supported by NIH Grant AM 32999. We thank Dr. Tom Chung for his assistance.

Appendix

Linearly Related First-Order Kinetics. For a sequence of reactions which are first order or, because of a large excess of reagents, can be put into pseudo-first-order conditions, a linear algebraic approach is effective.

Baldwin Model for Transferrin. (1) Let c_i represent the concentration of the species corresponding to reactions: $c_1 = Fe_aTfFe_b$, $c_2 = TfFe_b$, $c_3 = Fe_aTf$, $c_4 = Tf$, and $\mathbf{c}$ is the four-dimensional vector of these concentrations.

(2) For $d\mathbf{c}/dt$ we have the individual linear differential equations summarized by the information from the Baldwin scheme. This gives us $d\mathbf{c}/dt = \mathbf{Ac}$ where $\mathbf{A}$ is a 4 × 4 matrix containing the rate constants $dc_1/dt = -(k_{1a} + k_{1b})c_1$, $dc_2/dt = k_{1a}c_1 - k_{2b}c_2$, $dc_3/dt = k_{1b}c_1 - k_{2a}c_3$, and $dc_4/dt = k_{2b}c_2 + k_{2a}c_3$.

$$\mathbf{A} = \begin{bmatrix} -(k_{1a} + k_{1b}) & 0 & 0 & 0 \\ k_{1a} & -k_{2b} & 0 & 0 \\ k_{1b} & 0 & -k_{2a} & 0 \\ 0 & k_{2b} & k_{2b} & 0 \end{bmatrix}$$

(3) Now consider a trial solution $\mathbf{c} = \mathbf{Xv}$ where $\mathbf{v}$ is a vector of exponentials with $v_j = e^{-m_j t}$ and $\mathbf{X}$ is a 4 × 4 square array of coefficients. We assume that $\mathbf{X}$ is nonsingular.

$$\mathbf{v} = \begin{bmatrix} e^{-m_1 t} \\ e^{-m_2 t} \\ e^{-m_3 t} \\ e^{-m_4 t} \end{bmatrix}$$

(4) $d\mathbf{v}/dt = -\mathbf{Mv}$ where $\mathbf{M}$ is a diagonal matrix with $M_{jj} = m_j$.

$$\mathbf{M} = \begin{bmatrix} m_1 & 0 & 0 & 0 \\ 0 & m_2 & 0 & 0 \\ 0 & 0 & m_3 & 0 \\ 0 & 0 & 0 & m_4 \end{bmatrix}$$

(5) $d\mathbf{c}/dt = d(\mathbf{Xv})/dt = \mathbf{X}\, d\mathbf{v}/dt = -\mathbf{XMv}$.

(6) $d\mathbf{c}/dt = \mathbf{Ac} = \mathbf{AXv} = -\mathbf{XMv}$.

(7) $(\mathbf{AX} + \mathbf{XM})\mathbf{v} = \mathbf{0}$ implies $\mathbf{AX} = -\mathbf{XM}$ and if $\mathbf{X}$ is nonsingular then (8) is true.

(8) $|\mathbf{A} + \mathbf{M}| = \mathbf{0}$.

We now solve this determinant to get the m_j values as eigenvalues. Since $\mathbf{A} + \mathbf{M}$ is lower triangular, the determinant is the product of the diagonal elements. This implies the solutions (eigenvalues) are $m_1 = k_{1a} + k_{1b}$, $m_2 = k_{2b}$, $m_3 = k_{2a}$, and $m_4 = 0$.

(9) We next get products $\mathbf{AX}$ and $-\mathbf{XM}$ and use this to solve for $\mathbf{X}$, $\mathbf{AX} = -\mathbf{XM}$, using boundary conditions. If we let

$$q_1 = \frac{k_{1a}}{m_2 - m_1}$$

$$q_2 = \frac{k_{1b}}{m_3 - m_1}$$

and

$$q_3 = \frac{1}{m_1}\left(\frac{m_2}{m_1 - m_2} + \frac{m_3}{m_1 - m_3}\right)$$

(10) $\mathbf{c} = \mathbf{Xv}$ is the integrated form of the rate equation. At $t = 0$

$$\mathbf{c} = \begin{bmatrix} c_0 \\ 0 \\ 0 \\ 0 \end{bmatrix} \quad \mathbf{v} = \begin{bmatrix} 1 \\ 1 \\ 1 \\ 1 \end{bmatrix}$$

and at $t = \infty$

$$v = \begin{bmatrix} 0 \\ 0 \\ 0 \\ 1 \end{bmatrix} \qquad c = \begin{bmatrix} 0 \\ 0 \\ 0 \\ 2c_0 \end{bmatrix}$$

from $\mathbf{c} = \mathbf{Xv}$ (eq 9). Note that $q_1 + q_2 + q_3 = -1$ and that $k_{1a} = (m_2 - m_1)q_1$ and $k_{1b} = q_2(m_3 - m_1)$. So that we solve for the remaining elements of $\mathbf{X}$ to get

$$\mathbf{X} = \begin{bmatrix} c_0 & 0 & 0 & 0 \\ q_1 c_0 & -q_1 c_0 & 0 & 0 \\ q_2 c_0 & 0 & -q_2 c_0 & 0 \\ q_3 c_0 & q_1 c_0 & q_2 c_0 & c_0 \end{bmatrix}$$

where $c_1 = c_0 e^{-m_1 t}$, $c_2 = [k_{1a}c_0/(m_2 - m_1)][e^{-m_1 t} - e^{-m_2 t}]$, $c_3 = [k_{1b}c_0/(m_3 - m_1)][e^{-m_1 t} - e^{-m_3 t}]$, and $c_4 = c_0[1 + q_3 e^{-m_1 t} + q_1 e^{-m_2 t} + q_2 e^{-m_3 t}]$.

(39) Binford, J. S.; Foster, J. C. *J. Biol. Chem.* **1974**, *249*, 407–412.

Registry No. 3,4-LICAMS, 71353-11-2; Fe, 7439-89-6.